Engineering Experiment Station

ADVANCED STUDY OF VIDEO SIGNAL PROCESSING IN LOW SIGNAL TO NOISE ENVIRONMENTS

By

Frank Carden
Robert Henry

A Semi-Annual Progress Report

Submitted to

NATIONAL AERONAUTICAL SPACE ADMINISTRATION
WASHINGTON, D. C.

NASA RESEARCH GRANT NGR-32-003-037

Electrical Engineering Department
Communication Research Group

Dec. 1971 - May 1972

ADVANCED STUDY OF VIDEO SIGNAL PROCESSING IN LOW SIGNAL TO NOISE ENVIRONMENTS

By

Frank Carden
Robert Henry

A Semi-Annual Progress Report

Submitted to

NATIONAL AERONAUTICAL SPACE ADMINISTRATION
WASHINGTON, D. C.

NASA RESEARCH GRANT NGR-32-003-037

Electrical Engineering Department
Communication Research Group

June 1971 - November 1971

ABSTRACT

In this paper a non-linear analysis of a M PLL by using the method of "Harmonic Balance" is presented. The particular M PLL considered has a low-pass filter and a band-pass filter in parallel. An analytic expression for the relationship between the input signal phase deviation and the phase error is determined for sinusoidal FM in the absence of noise. The expression is used to determine bounds on the proper operating region for the M PLL and to investigate the "Jump Phenomenon" previously observed. From these results the proper modulation index, modulating frequency, etc. used for the design of a M PLL is determined. Data for the loop unlock boundary obtained from the theoretical expression are compared to data obtained from analog computer simulations of the M PLL.

I. INTRODUCTION

The phase-lock loop (PLL) has become more widely used as an FM demodulator in the past several years. This is due to the superior noise rejection properties and threshold extension exhibited by the PLL. These properties are particularly useful in aerospace frequency modulation (FM) communication systems where receivers must operate in low signal-to-noise-ratio environments. However, the common low-pass PLL will yield little or no threshold improvement over the conventional FM discriminator when the spectrum of the demodulated FM signal contains information at or near discreet frequencies in addition to the baseband signal. This is a characteristic of the typical IRIG spectrum. The Apollo unified S-band communication system is also such a system. It has a spectrum (see Fig. 1) which consists of wide-band information at baseband and narrowband information on a subcarrier. In this case the low-pass PLL allows noise in the unused portion of the bandwidth to enter the loop and thus lowers the loop signal-to-noise ratio. This problem is further compounded by poorer tracking performance of the low-pass PLL when relatively high-energy subcarriers occur in the upper part of the passband.

A solution to this problem involves the use of additional filters in the loop in parallel with the low-pass filter [4]. This type of PLL is called a multifilter PLL (M PLL). The frequency response of such a M PLL matched to the above mentioned spectrum is shown in Fig. 1 along with the conventional low-pass PLL.

Recently there has been an interest in a comparison between the multifilter phase feedback loop (M PFL), as used in precision ranging

systems [5], and the M PLL. It has been shown [6] that the parameters and filter responses of the M PFL and the M PLL are related. By using these relations the M PFL performance characteristics can be determined by the performance characteristics of an equivalent M PLL. Therefore the result of this paper can be applied to the M PFL as well as to the M PLL.

In this paper a non-linear analysis of a M PLL is presented. The particular M PLL considered has a low-pass filter and a band-pass filter in parallel. An analytic expression for the relationship between the input signal phase deviation and the phase error is determined for sinusoidal FM in the absence of noise. The expression is used to determine bounds on the proper operating region for the M PLL and to investigate the "Jump Phenomenon" previously observed [2]. From these results the proper modulation index, modulating frequency, etc. used for the design of a M PLL is determined. Data for the loop unlock boundary obtained from the theoretical expression are compared to data obtained from analog computer simulations of the M PLL.

II. THE M PLL DIFFERENTIAL EQUATION

The Carrier Model of a typical phase-lock loop (PLL) is illustrated in Fig. 2. The phase detector generates an error voltage which is a function of the phase difference (error) between the input signal and the VCO (Voltage Controlled Oscillator) output. This error voltage is then used (after filtering) to modify the VCO output so as to reduce the phase error. Thus the VCO attempts to "track" the input signal. Since the VCO input is proportional to the VCO output frequency, the loop filter output is proportional to the input signal frequency (when the PLL is "tracking" the input signal).

Viterbi [1] has reduced the Carrier Model to a baseband or phase model for the case in which the phase detector is simply an ideal multiplier (assuming harmonics of the carrier frequency are filtered out). This model is shown in Fig. 3(a) where the loop gain is assumed to be included in the loop filter.

Assume that F(s) is a linear filter with a rational transfer function given by

$$F(s) = \frac{a_o + a_1 s + a_2 s^2 + \ldots . a_m s^m}{b_o + b_1 s + b_2 s^2 + \ldots . b_n s^n} \tag{1a}$$

where $m \leq n$. It can be shown [1] that the PLL operation is described by the differential equation

$$(b_o + b_1 p + \ldots . b_n p^n)[\dot{\phi}(t) - \dot{\theta}_1(t)]$$

$$= -A(a_o + a_1 p + \ldots . + a_m p^m) \sin \phi(t) \tag{1b}$$

where p is an operator indicating differentiation.

The phase model of a multi-filter phase-lock loop (M PLL) with a low-pass filter (LPF) and a band-pass filter (BPF) in parallel is shown in Fig. 3(b). This is just an extension of the model in Fig. 3(a).

The LPF is necessary in order that the M PLL track the carrier. The filter used in this study is one with a single pole transfer function given by

$$F_1(s) = 1 + \frac{a}{s} = \frac{s + a}{s} . \tag{2a}$$

Cheng [2] has shown that a desirable BPF is a tuned-loop filter followed by a differentiator. It has a transfer function given by

$$F_2(s) = \frac{s^2}{s^2 + 2\zeta_o\omega_o s + \omega_o^2} . \tag{2b}$$

Comparing Fig. 3(b) with 3(a) yields

$$F(s) = A_1F_1(s) + A_2F_2(s) \tag{2c}$$

and A = 1. Substituting (2a) and (2b) into (2c)

$$F(s) = \frac{A_1(s + a)}{s} + \frac{A_2s^2}{s^2 + 2\zeta_o\omega_o s + \omega_o^2}$$

$$= \frac{(A_1 + A_2)s^3 + A_1(a + 2\zeta_o\omega_o)s^2 + A_1(2\zeta_o\omega_o a + \omega_o^2)s + A_1a\omega_o^2}{s^3 + 2\zeta_o\omega_o s^2 + \omega_o^2 s} \tag{2d}$$

Comparison of Equation (2d) and (1a) yields

$$\left.\begin{aligned} a_o &= A_1\omega_o^2 a & b_o &= 0 \\ a_1 &= A_1(2\zeta_o\omega_o a + \omega_o^2) & b_1 &= \omega_o^2 \\ a_2 &= A_1(a + 2\zeta_o\omega_o) & b_2 &= 2\zeta_o\omega_o \\ a_3 &= A_1 + A_2 & b_3 &= 1 \end{aligned}\right\} \quad (2e)$$

By applying the operator, Equation (1b) yields the following differential equation for the M PLL:

$$\boxed{\begin{aligned} &b_1\ddot{\phi} + b_2\dddot{\phi} + b_3\ddddot{\phi} + a_o\sin\phi + a_1\dot{\phi}\cos\phi + a_2(\ddot{\phi}\cos\phi - \dot{\phi}^2\sin\phi) \\ &\quad + a_3[(\dddot{\phi} - \dot{\phi}^3)\cos\phi - 3\ddot{\phi}\,\dot{\phi}\sin\phi] = b_1\ddot{\theta}_1 + b_2\dddot{\theta}_1 + b_3\ddddot{\theta}_1 \end{aligned}} \quad (2f)$$

It is understood that ϕ and θ_1 are functions of time.

III. SOLUTION OF THE M PLL DIFFERENTIAL EQUATION

The input signal will be assumed to be a carrier frequency modulated by a single sinusoid. This corresponds to

$$\theta_1 = \beta\cos(\omega_m t + \lambda) \tag{3a}$$

where $\beta = \Delta\omega/\omega_m$ is the peak input phase deviation, ω_m is the modulating frequency, and λ is a phase shift relative to the phase of ϕ. It is not unreasonable to expect that ϕ is a sinusoid of frequency ω_m since θ_1 and θ_2 are sinusoidal as long as the loop is locked (tracking θ_1). That ϕ is sinusoidal has in fact been observed from analog computer simulations of the M PLL. Thus it is assumed that the loop is locked and the phase error is given by

$$\phi = P\ \sin(\omega_m t) \tag{3b}$$

where P is the peak phase error.

There is no known exact solution to the non-linear 4th order differential equation given by Equation (2f). However, under the above assumptions the steady-state conditions of the solution may be determined by the Principle of Harmonic Balance [3]. Essentially this method consists of adjusting the solution parameters so that fundamental components fit the non-linear equation as best as possible.

Substitution of Equation (3a) into the right side of Equation (2f) yields

$$\begin{aligned} EXR &= \beta C\ \sin(\omega_m t + \lambda) - \beta B\ \cos(\omega_m t + \lambda) \\ &= \beta[C\ \cos\lambda + B\ \sin\lambda]\ \sin(\omega_m t) + \beta[C\ \sin\lambda - B\ \cos\lambda]\ \cos(\omega_m t) \end{aligned} \tag{3c}$$

where

$$\boxed{C = b_2\omega_m^3} \quad \text{and} \quad \boxed{B = b_1\omega_m^2 - b_3\omega_m^4} \tag{3d}$$

and EXR means expansion of the right side of (2f).

Substitution of Equation (3b) into the left side of Equation (2f) and using the Bessel Function expansions [7]

$$\cos(P\sin(\omega t)) = J_o(P) + 2[J_2(P)\cos(2\omega t) + J_4(P)\cos(4\omega t) + \ldots]$$
$$\sin(P\sin(\omega t)) = 2[J_1(P)\sin(\omega t) + J_3(P)\sin(3\omega t) + \ldots] \tag{3e}$$

yields the following expansion for the left side of (2f) (EXL)

$$\begin{aligned} EXL = {} & 2[J_1(P)\sin(\omega_m t) + J_3(P)\sin(3\omega_m t) + \ldots.][a_o - a_2P^2\omega_m^2\cos^2(\omega_m t) \\ & + 3a_3P^2\omega_m^3\sin(\omega_m t)\cos(\omega_m t)] + \{J_o(P) + 2[J_2(P)\cos(2\omega_m t) \\ & + J_4(P)\cos(4\omega_m t) + \ldots.]\}\, P[a_1\omega_m\cos(\omega_m t) - a_2\omega_m^2\sin(\omega_m t) \\ & + a_3\omega_m^3(\cos(\omega_m t) + P^2\cos^3(\omega_m t))] \end{aligned} \tag{3f}$$

By using trigonometric identities in (3f) and collecting common terms for $\cos(\omega_m t)$ and $\sin(\omega_m t)$, Equation (3f) becomes

$$\begin{aligned} EXL = {} & P[-b_2\omega_m^3 - a_3\omega_m^3\{J_o(P) + J_2(P) - \tfrac{3P}{2}(J_1(P) + J_3(P)) + \tfrac{P^2}{4}(3J_o(P) \\ & + 4J_2(P) + J_4(P))\} + a_1\omega_m\{J_o(P) + J_2(P)\}]\cos(\omega_m t) \\ & + P[\omega_m^2\{b_3\omega_m^2 - b_1\} + a_2\omega_m^2\{-J_o(P) + (\frac{2a_o}{a_2P\omega_m^2} - \frac{P}{2})J_1(P) + J_2(P) \\ & - PJ_3(P)\}]\sin(\omega_m t) + H.O.T \end{aligned} \tag{3g}$$

where H.O.T. indicates the higher order terms - ~~$\sin^2(\omega_m t)$, $\cos^2(\omega_m t)$,~~ $\sin 2\omega_m t$, $\cos 2\omega_m t$, ~~$\sin^3(\omega_m t)$~~ $\sin 3\omega_m t$, etc.

Equating the coefficients of $\sin(\omega_m t)$ and $\cos(\omega_m t)$ in Equations (3h) and (3c) gives

$$\beta[C\cos(\lambda) + B\sin(\lambda)] = K_1$$

$$\beta[C\sin(\lambda) - B\cos(\lambda)] = K_2 \qquad (3h)$$

where

$$K_1 = P[\omega_m^2\{b_3\omega_m^2 - b_1\} + a_2\omega_m^2\{-J_o(P) + (\frac{2a_o}{a_2 P\omega_m^2} - \frac{P}{2})J_1(P) + J_2(P) - PJ_3(P)\}] \qquad (3i)$$

and

$$K_2 = P[-b_2\omega_m^3 - a_3\omega_m^3\{J_o(P) + J_2(P) - \frac{3P}{2}(J_1(P) + J_3(P)) + \frac{P^2}{4}(3J_o(P) + 4J_2(P) + J_4(P))\} + a_1\omega_m\{J_o(P) + J_2(P)\}]$$

By using the trigonometric identity

$$\sin^2(\lambda) + \cos^2(\lambda) = 1$$

it is easy to show that (3h) yields

$$\beta^2 = \frac{K_1^2 + K_2^2}{C^2 + B^2} \qquad (3j)$$

and

$$\cos(\lambda) = \frac{\beta(K_1 C - K_2 B)}{C^2 + B^2} \qquad (3k)$$

Equation (3j) is the desired solution since it gives the relationship between the peak phase error (P) and the peak input signal phase deviation (β) in terms of the M PLL parameters and the modulating frequency.

IV. THE M PLL PHASE ERROR CHARACTERISTICS

A typical frequency response for the M PLL considered in this paper is shown in Figure 4(a). This response is for operation in the linear region of the M PLL - where $\sin\phi \simeq \phi$. It has been shown [2] that:

$$\left.\begin{aligned} A_1 &= 2\zeta_{cL1}\,\omega_{n1} \\ A_1 a &= \omega_{n1}^2 \end{aligned}\right\} \text{ for low-pass filter}$$

$$\left.\begin{aligned} \zeta_{cL2} &= \zeta_o + \frac{A_2}{2\omega_o} \\ &= \frac{BW_{3db}}{2\omega_o} \\ \omega_{n2} &= \omega_o \\ BW_{3db} &= 2\zeta_o\omega_o + A_2 \\ G &= \frac{A_2}{BW_{3db}} \end{aligned}\right\} \text{ for band-pass filter} \qquad (4a)$$

ζ_{cL} is the closed-loop damping ratio, ω_n is the natural frequency, BW_{3db} is the 3db bandwidth of the filter, and G is the peak amplitude of the BPF (occurs at $\omega_m = \omega_{n2}$) relative to the d.c. gain of the LPF.

A digital computer program was developed to determine values for β for various values of P and M PLL parameters using Equation (3j). A series expansion [7] was used to determine the Bessel Function to 0.01% accuracy.

The results for peak phase error of 1.5 radians (P = 1.5) using the same M PLL parameters as in Figure 4(a) is shown in Figure 4(b). Note

the rapid decrease in β as ω_m increases from ω_o to the 3db frequency. For values of ω_m removed from the influence of either the LPF or BPF, $\beta = P = 1.5$. This is to be expected since the M PLL does not track modulation outside of the filter response and the phase error equals the input phase. Also plotted are values for $A_1 = 0$ (the LPF removed) and for $A_2 = 0$ (the BPF removed). As can be seen the BPF has little effect on the values for frequencies near the LPF. Likewise the LPF has little effect on the values for frequencies near the BPF. The influence of the LPF extends to approximately 10 times the filter natural frequency. Thus if $\frac{\omega_o - BW_{3db}}{\omega_{n2}} > 10\omega_{n1}$ the two filters may be assumed not to interact and the appropriate equation (either with $A_1 = 0$ or $A_2 = 0$) may be used. The above results were also observed for values of P in the range from 0 to 3 radians.

By setting $A_1 = 0$ Equation (3j) may be simplified to yield results valid for ω_m in the BPF region (provided $\frac{\omega_o - BW_{3db}}{\omega_{n2}} > 10\omega_{n1}$). Setting $A_1 = 0$ in Equations (2e) and substituting these values into Equations (3d), (3i) and then into Equation (3j) gives

$$\beta^2 = \frac{(D\omega)^2 + (2\zeta_o + \frac{A_2}{\omega_o} K(P))^2}{(D\omega)^2 + 4\zeta_o^2} P^2 \qquad (4b)$$

where

$$D\omega \triangleq \frac{\omega_m^2 - \omega_o^2}{\omega_o \omega_m} = \frac{\omega_m}{\omega_o} - \frac{\omega_o}{\omega_m} \qquad (4c)$$

and

$$K(P) = [J_o(P) + J_2(P) - \frac{3P}{2}\{J_1(P) + J_3(P)\} + \frac{P^2}{4}\{3J_o(P) + 4J_2(P) + J_4(P)\}] \quad (4d)$$

Equation (4d) may be written in terms of $J_1(P)$ by using the recurrence formulas for the Bessel Functions [7],

$$\boxed{K(P) = \frac{2J_1(P)}{P}} \quad (4e)$$

From Equations (4a) it is easily shown that

$$\frac{A}{\omega_o} = 2\zeta_o \frac{G}{1 - G} . \quad (4f)$$

When this value is substituted into Equation (4b) it becomes

$$\boxed{\beta^2 = \frac{(D\omega)^2 + 4\zeta_o^2(1 + \frac{GK(P)}{1 - G})^2}{(D\omega)^2 + 4\zeta_o^2} P^2} \quad (4g)$$

V. THE JUMP PHENOMENON

Figure 5 shows typical plot of β vs. P as obtained from Equation (4b). The domain of P is restricted to $0 - \pi$ radians since $P > \pi$ causes sin P to be negative which in turn causes positive feedback in the M PLL and resulting loss of lock. Here we are interested in the characteristics during and before loss of lock. It is interesting to observe the behavior of P as β is increased for $D\omega = 0$ ($\omega_m = \omega_o$). For small β, P increases linearly; however, a point is reached (at $dB/dP = 0$) for which a further increase in β does not satisfy the equation for any P near this point.

At this point P "Jumps" to some value greater than π and results in loss of lock. This is the phenomenon observed by Carden, Thompson and Cheng [2]. It should also be noted that for $D\omega$ far enough removed from 0, the "Jump" phenomenon does not occur - the M PLL loses lock without a Jump in P. This can be more readily seen by referring to Figure 6. Data for this figure was obtained from Figure 5 and plotted for constant values of β. For $|D\omega| > 0.08$, and increase in β (holding $D\omega$ constant) is accompanied by an increase in P (in a non-linear manner) until the loop breaks lock. For $|D\omega| < 0.08$, an increase in β initially results in an increase in P until a point indicated by the dashed line is reached. At this point a further increase in β results in a "Jump" in P and loss of lock. The point at which the "Jump" occurs can be determined analytically by finding $d\beta/dP$ from Equation (4b) and setting this value equal to zero. The results of this procedure yields

$$2\left[4\zeta_o + \frac{2A}{\omega_o}\frac{J_1(P)}{P}\right]\frac{dJ_1(P)}{dP} = -\frac{\omega_o}{A}\left(D\omega^2 + 4\zeta_o^2\right) \qquad (4h)$$

The locus of points obtained from this equation is also plotted in Figure 6 and corresponds to the points at which the slope of the constant β lines is infinite. It should be noted that for a different ζ_o and G, Figure 5 and Figure 6 will have the same form but different numerical values. The figures of course can be obtained by plotting Equation (4g).

VI. COMPARISON WITH ANALOG COMPUTER RESULTS

An Analog Computer Simulation of the M PLL was set up on an EAI 680 Analog Computer. β was increased slowly and the resulting phase error was observed. Points were recorded when P equaled 1.5 and when the M PLL lost lock. This was done for various ω_m near ω_o and for BPF parameters ω_o = 10, BW = 1, G = .85; ω_o = 10, BW = 2, G = .85; ω_o = 10, BW = 4, G = .85; and ω_o = 5, BW = 2.0, G = .95. The LPF BW_{3db} = .1 and ζ = .707 for all cases. The phenomenon of "Jumps" was observed as the M PLL lost lock for ω_m near ω_o.

The results of the analog computer simulation are plotted in Figures 7(a) through 7(d) along with the values predicted by Equation (4g). The values for loop unlock using the equation were obtained from a plot similar to that of Figure 5. For $D\omega$ near ω_o (where "Jumps" occur) β was the value at which $d\beta/dP = 0$. For the other $D\omega$ (where "Jumps" do not occur) β was the value which corresponds to a P of 2.5 radians. This was found to be the phase error for which the M PLL lost lock for ω_m where there are no jumps. As can be seen, the results agree to within about 10% for all cases. The analog computer readings were never greater than the values predicted by Equation (4g). This may be partially due to noise associated with the analog computer components. The assumption of neglecting the higher harmonic components in the solution to the differential equation is therefore not very restrictive (at least for the cases considered here).

Equation (4g) indicates that the loop unlock characteristics are a function of ω_m/ω_n (actually $D\omega$) if G (peak gain of BPF) and ζ_o (open loop damping ratio associated with BPF) remain the same. Normally G is made

as close to 1 as possible so that the output voltage in the BPF region is well above the noise level. Thus a plot (with ω_m normalized by ω_n) for $\omega_o = 5$, BW = 1 gives the same results as a plot for those values doubled ($\omega_1 = 10$, BW = 2) provided the same G and ζ_o is maintained. This applies to the results indicated in Figure 6 as well, since those results were derived from Equation (4g). Note that the Q of the filter is the same in both cases indicating that the M PLL characteristics are related to the energy stored in the filter.

VII. CONCLUSION

The derived equations predict that a "Jump" Phenomenon exists for ω_m near the center of the BPF region. The "Jump" in phase is larger for ω_m closer to the center of frequency. Numerical values agree to within 10% of values obtained from analog computer simulations.

In order to avoid the "Jumps" in phase (and resulting loss of lock) an operational and design constraint is that β be kept well below the values at which this phenomenon occurs. It was observed from analog computer simulations that negligible distortion of the signal occurs for $P < 1.5$. Thus a desirable region of operation for the M PLL is that region below the $P = 1.5$ line in Figures 7(a), 7(b), 7(c) and 7(d). From these figures it is also evident that the subcarrier must be accurately centered in the BPF region since the maximum allowable β decreases rapidly as ω_m is increased or decreased toward the 3db frequencies.

If the center frequency of the BPF and the 3db frequency of the LPF are at least one decade apart the filters do not interact. Equation (4g) and its associated plots may then be conveniently used in the design of a M PLL. Assuming that ζ_o and G remain unchanged from design to design, Equation (4g) may be used to generate a single plot of β vs. $D\omega$ to be used in the design process. BPF's with the same Q (ω_o/BW_{3db}) have identical characteristics when plotted as a function of $D\omega$.

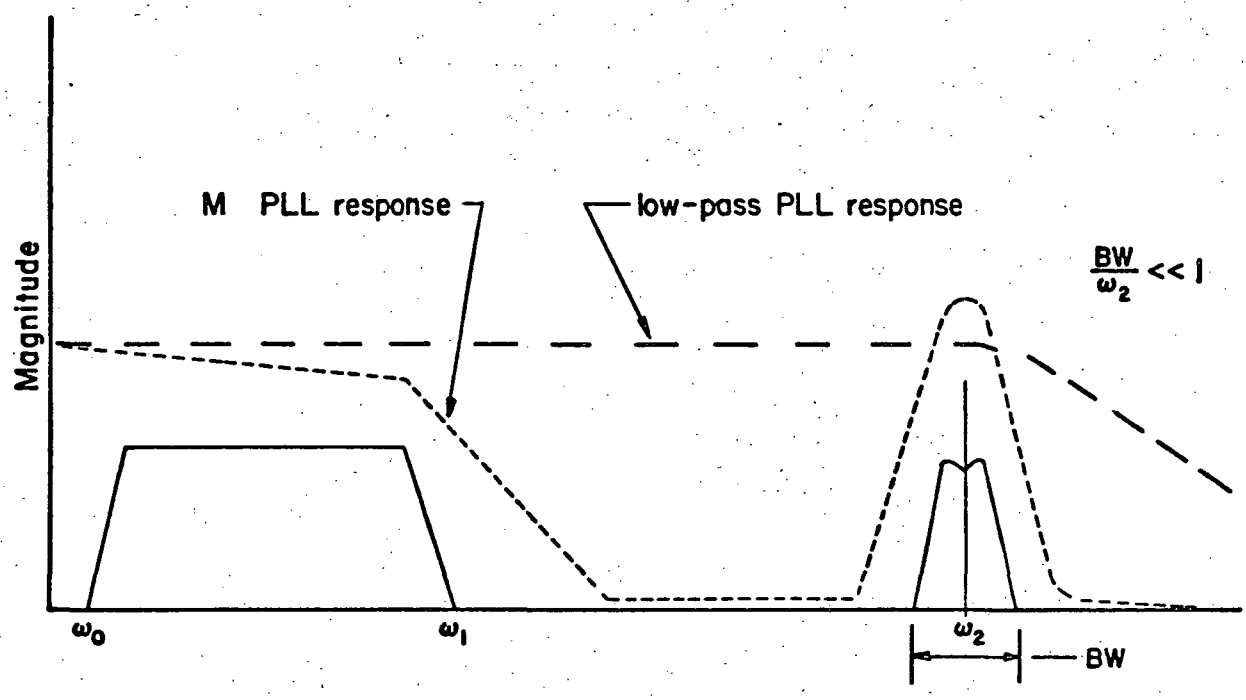

Fig. 1. Typical Apollo unified S-band spectrum (baseband) with frequency responses of a PLL and M PLL used for its demodulation.

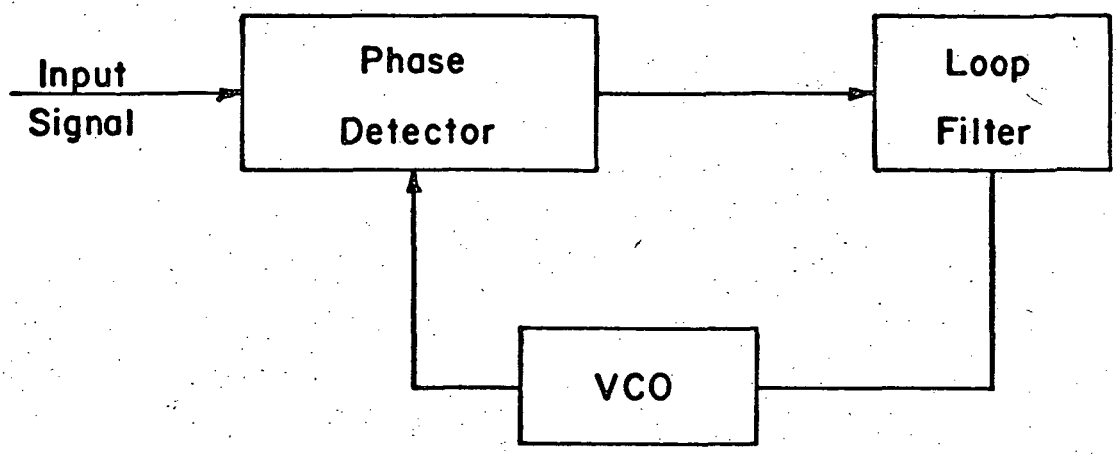

Fig. 2. The Carrier Model of a PLL.

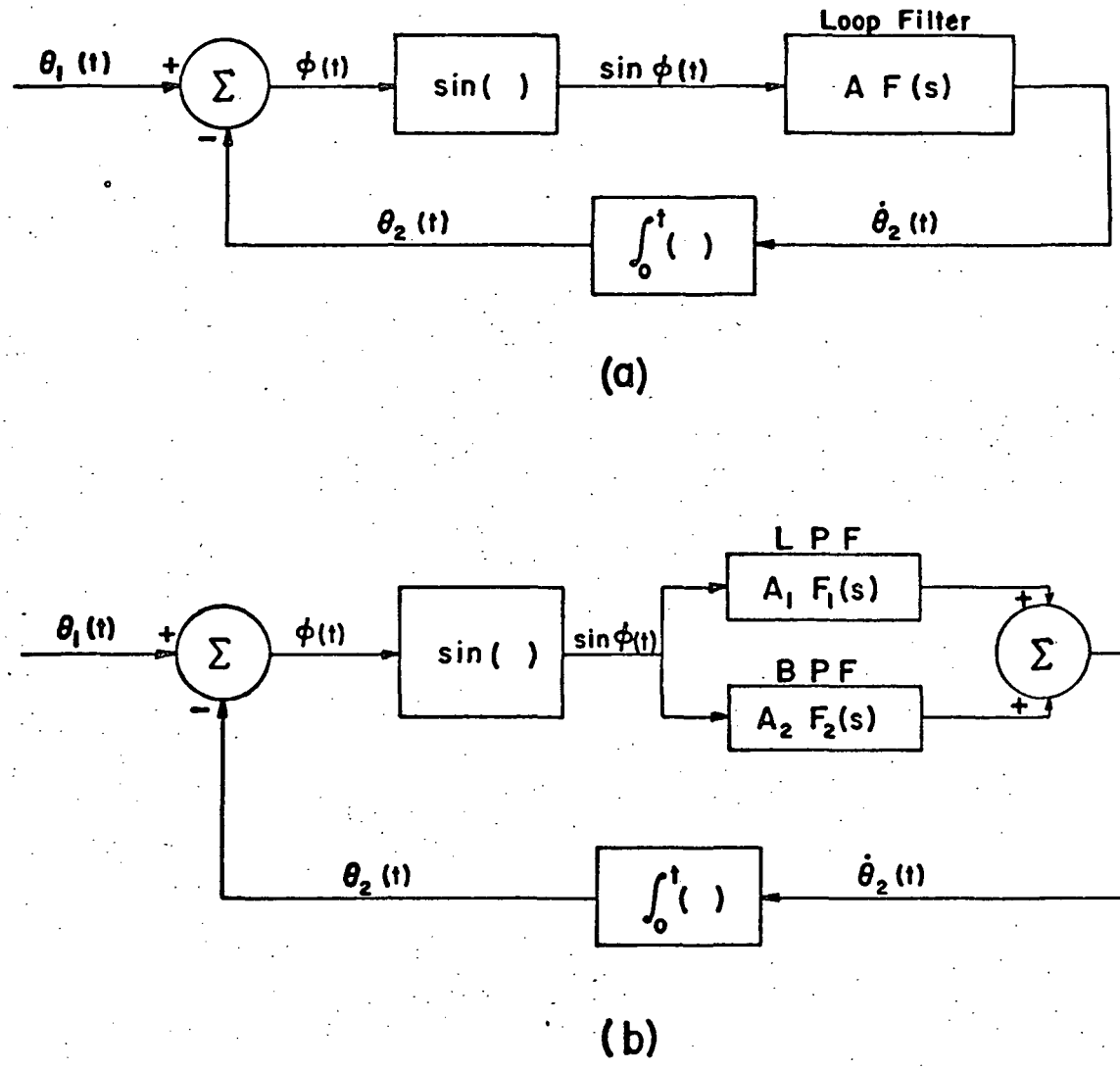

Fig. 3. (a) The Phase Model of a PLL.
(b) The Phase Model of a M PLL.

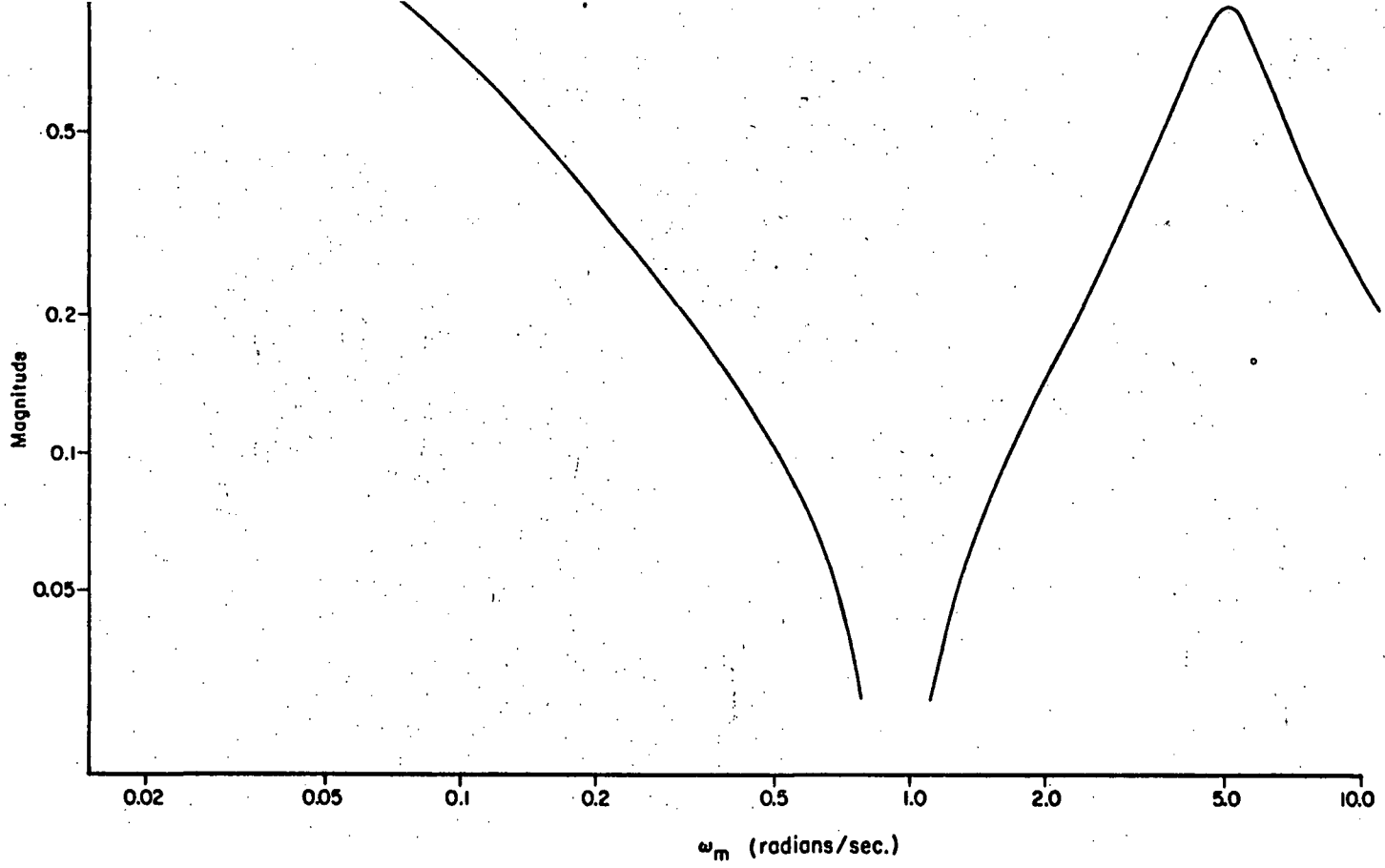

Fig. 4(a). Overall closed-loop frequency response of the M PLL for $A_1 = 0.0707$, $a = 0.0354$, ($BW_{3db} = 0.1$, $\zeta_{CL1} = 0.707$); $A_2 = 1.9$, $\omega_o = 5.0$, $\zeta_{OL2} = 0.01$, ($BW_{3db} = 2.0$, $\zeta_{CL2} = 0.2$, $G = 0.95$).

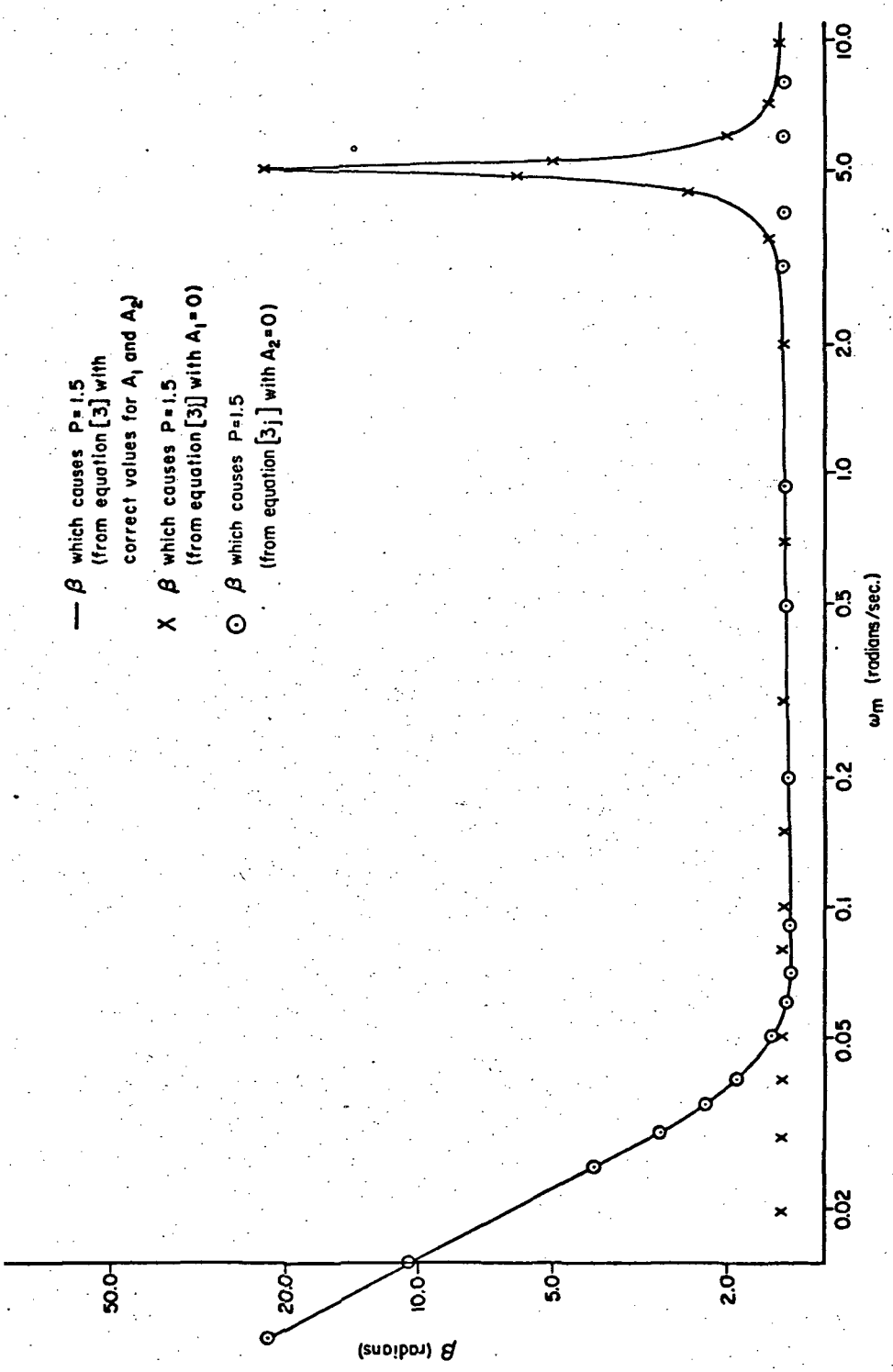

Fig. 4(b). β vs. ω_m for P = 1.5, A_1 = 0.0707, a = 0.0354, A_2 = 1.9, ω_o = 5.0, ζ_{OL2} = 0.01.

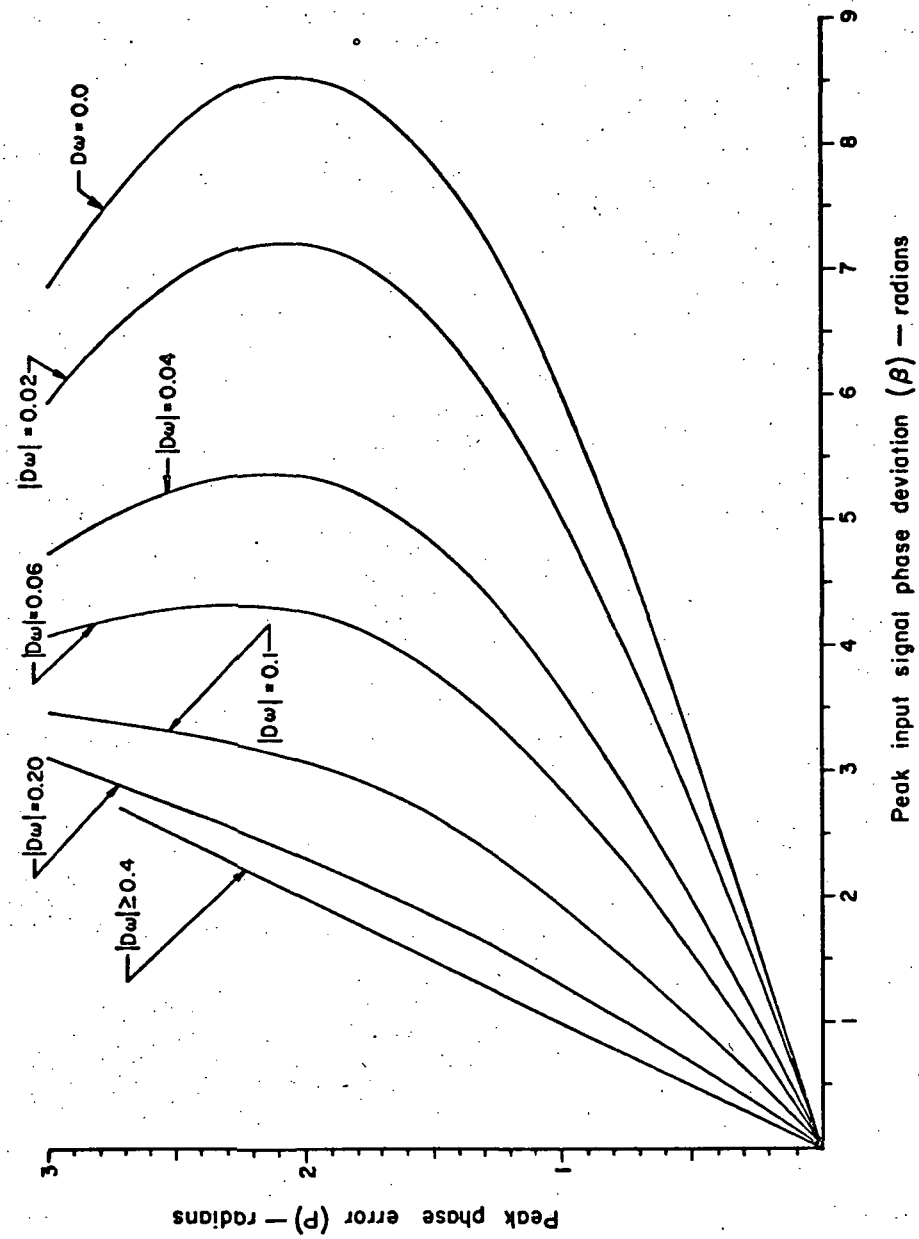

Fig. 5. Typical plot of β vs. P

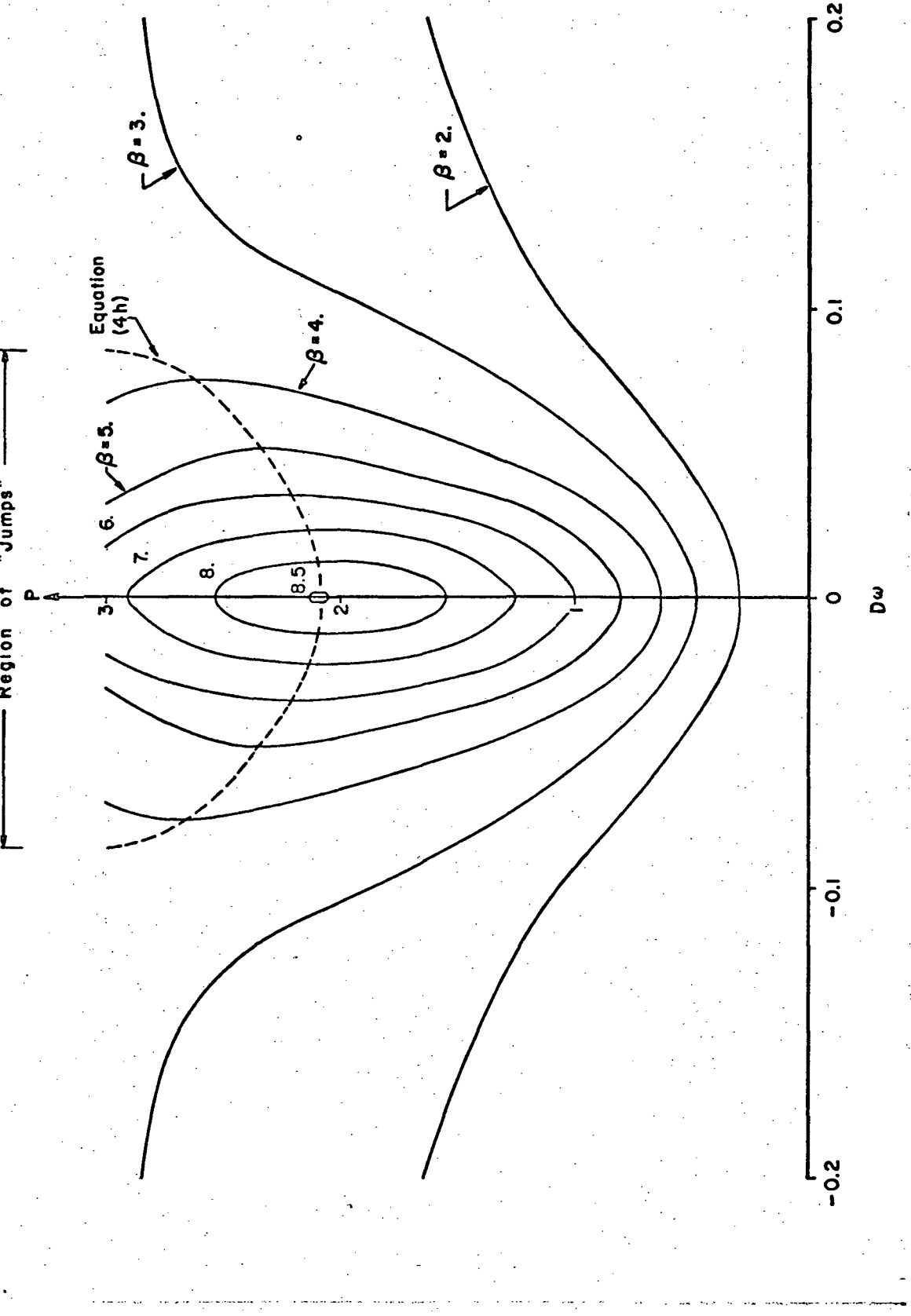

Fig. 6. Typical plot of Dω vs. P. $\zeta_o = 0.015$, $\omega_o = 10.0$, $A_2 = 1.7$.

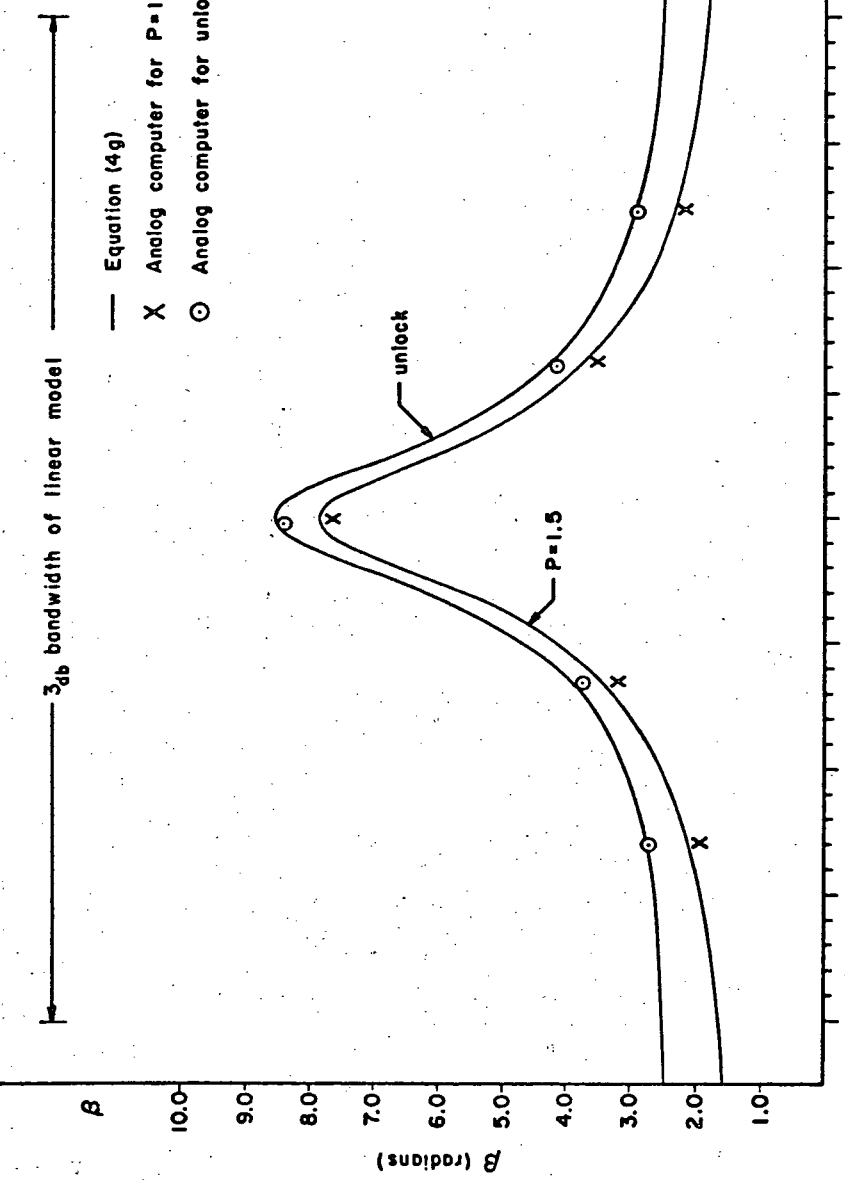

Fig. 7(a). β vs. $D\omega$. $\zeta_o = 0.03$, $\omega_o = 10.0$, $A_2 = 3.4$, ($G = 0.85$, $BW = 4.0$).

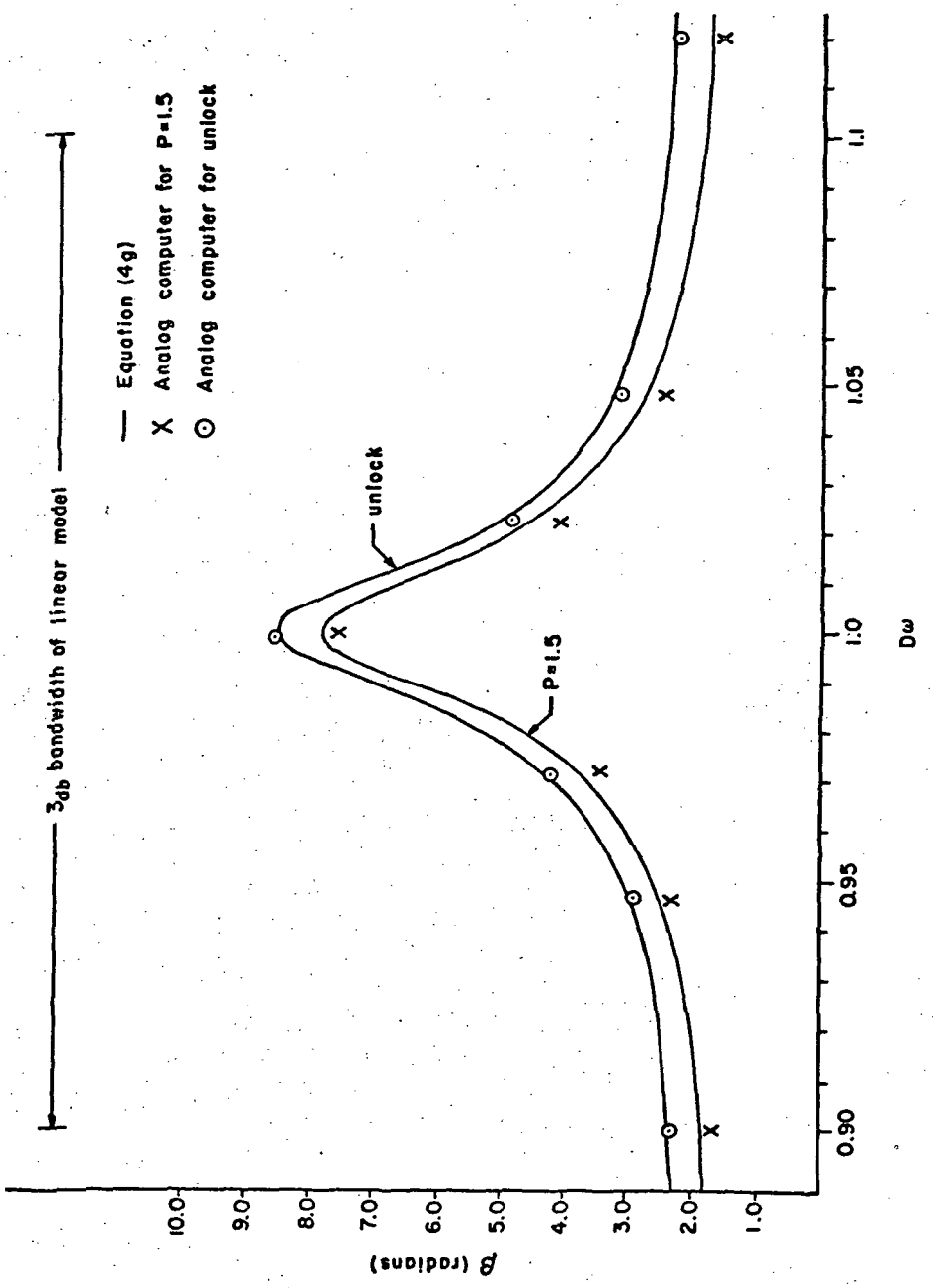

Fig. 7(b). β vs. $D\omega.\zeta_o = 0.015$, $\omega_o = 10.0$, $A_2 = 1.7$; ($G = 0.85$, $BW = 2.0$).

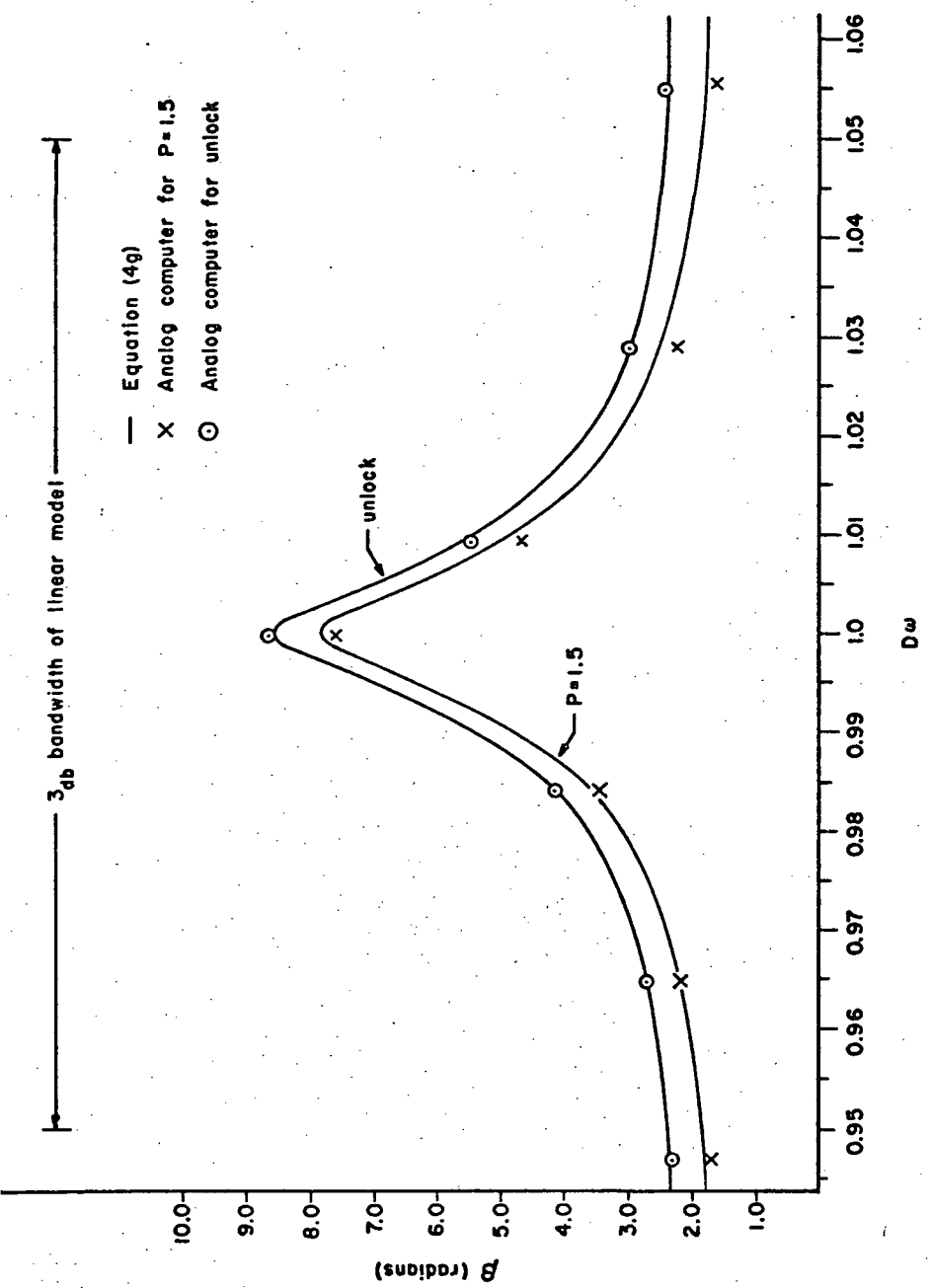

Fig. 7(c). β vs. $D\omega.\zeta_o = 0.0075$, $\omega_o = 10.0$, $A_2 = 0.85$, (G = 0.85, BW = 1.0).

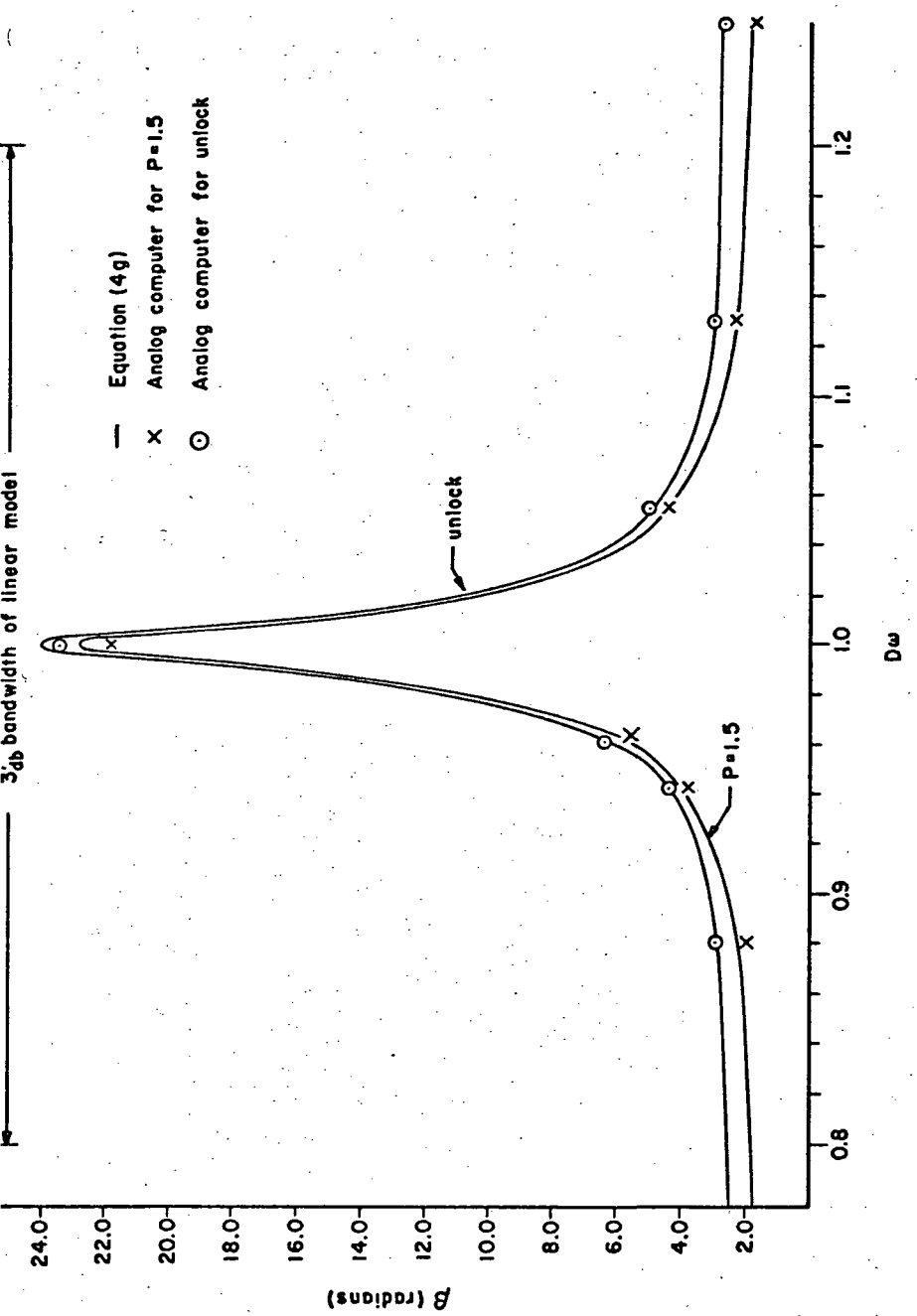

Fig. 7(d). β vs. $D\omega.\zeta_o = 0.01$, $\omega_o = 5.0$, $A_2 = 1.9$, ($G = 0.95$, $BW = 2.0$).

REFERENCES

[1] A. J. Viterbi, Principles of Coherent Communication. New York: McGraw-Hill Book Company, Inc., 1966.

[2] F. F. Carden, W. E. Thompson, and E. Cheng, "A Multifilter Phase-Lock Loop," IEEE Trans. Commun. Technol., Vol. 19, Part I, pp. 669-675, October 1971.

[3] W. J. Cunningham, Introduction to Nonlinear Analysis. New York: McGraw-Hill Book Company, Inc., 1958.

[4] R. P. Liccini, "FM Signal Data Demodulation System Analysis," TRW Syst., Monthly Prog. Rep., Jan. 31, 1968.

[5] R. J. Panneton, "General Operation of CIRIS Radio Reference Subsystem," TRW IOC No. 71:7151. RJP-382, September 2, 1971.

[6] R. J. Panneton, "A Multifilter Phase Feedback Loop - A Comparison," TRW Syst., IOC No. 72:7153.6-7, January 20, 1972.

[7] "Handbook of Mathematical Functions with Formulas, Graphs, and Mathematical Tables," U. S. Dept. of Commerce, National Bureau of Standards, May 1968.